T2R2 東京科学大学 リサーチリポジトリ
Science Tokyo Research Repository

論文 / 著書情報
Article / Book Information

Title	Centrifuge model tests on suffusion-induced deterioration and its consequences in seismic response of levees
Authors	Akihiro Takahashi, Tamaki Inoue, Saki Yamagata, Kazuki Horikoshi
Citation	Soils and Foundations, Vol. 65, Issue 2, 101592
Pub. date	2025, 3
DOI	https://doi.org/10.1016/j.sandf.2025.101592
Creative Commons	Information is in the article.

Powered by T2R2 (Science Tokyo Research Repository)

HOSTED BY
ELSEVIER
Available online at www.sciencedirect.com
ScienceDirect
Soils and Foundations 65 (2025) 101592
www.elsevier.com/locate/sandf

Centrifuge model tests on suffusion-induced deterioration and its consequences in seismic response of levees ☆

Akihiro Takahashi [a,*], Tamaki Inoue [b], Saki Yamagata [c], Kazuki Horikoshi [d]

[a] Department of Civil and Environmental Engineering, Institute of Science Tokyo, 2-12-1 O-okayama, Meguro, Tokyo 152-8550, Japan
[b] Tokyo Metro (Formerly, Tokyo Institute of Technology), Japan
[c] JFE Engineering (Formerly, Tokyo Institute of Technology), Japan
[d] Graduate School of Technology, Industrial and Social Sciences, Tokushima University, Japan

Received 19 August 2024; received in revised form 27 November 2024; accepted 11 February 2025

Abstract

Shake table tests on a levee deteriorated by seepage-induced internal erosion are performed in a geotechnical centrifuge to investigate the effects of erosion-induced heterogeneity and mechanical characteristics change on the seismic response of the levee. Among the several forms of internal erosion, suffusion, in which the seepage-induced loss of soil integrity occurs with the migration and loss of finer particles, is the focus of this study, since it progresses and puts structures in danger, while going unnoticed. In the tests, the model levee made of gap-graded soil is firstly subjected to repeated seepage flow by changing the water level in the flood channel. After lowering the water level and making the levee dry, earthquake motions are applied to the model deteriorated by suffusion. The progression of suffusion in the levee is confirmed by comparing the results of tests having the same initial condition, but subjected to a different number of seepage cycles. The shake table tests reveal that the natural frequency of the levee and the equivalent shear wave velocity in the levee significantly decrease with suffusion, suggesting that a reduction in soil stiffness occurs due to suffusion. However, no significant difference can be confirmed in the earthquake-induced crest settlement depending on the seepage cycles, suggesting that no marked change in strength or cyclic-shearing-induced compression occurs with suffusion within the scope of this study.
© 2025 Production and hosting by Elsevier B.V. on behalf of The Japanese Geotechnical Society. This is an open access article under the CC BY-NC-ND license (http://creativecommons.org/licenses/by-nc-nd/4.0/).

Keywords: Levee; Internal erosion; Suffusion; Centrifuge modelling; Shake table test

1. Introduction

Repeated water seepage over a long period causes the internal erosion of earthen structures. This internal erosion leads to the migration and loss of soil particles inside the earthen structures or under the ground. For this reason, internal erosion makes the soil looser or creates voids in the structures/ground, leading to the deterioration of the soil and the degradation of the stability of the structures over time. Internal erosion progresses gradually inside earthen structures or under the ground and its progression typically goes unnoticed. Even without obvious traces, internal erosion can be a predisposing factor for the instability of earthen structures. Thus, the causal relationship between internal erosion and earthen structure failure cannot be easily identified.

Foster and Fell (1999) proposed a four-phase failure path diagram for failure due to backward erosion piping (or simply piping) through embankment dams: (1) initiation of erosion, (2) continuation of erosion, (3) progression to the formation of a pipe, and (4) formation of a breach mechanism. They described this internal erosion process by detailed event trees. While the last two phases are related to piping, with visible traces of internal erosion occurring in a short period, the first two phases correspond

☆ This article is part of a special issue entitled: '8ICEGE-Osaka 2024' published in Soils and Foundations.

* Corresponding author.
E-mail address: takahashi.a.3a81@m.isct.ac.jp (A. Takahashi).

https://doi.org/10.1016/j.sandf.2025.101592
0038-0806/© 2025 Production and hosting by Elsevier B.V. on behalf of The Japanese Geotechnical Society.
This is an open access article under the CC BY-NC-ND license (http://creativecommons.org/licenses/by-nc-nd/4.0/).

to the above-mentioned long-term process. For most of their service life, earthen structures are exposed to repeated seepage that causes the first two phases of internal erosion. Therefore, to assess the failure risk of earthen structures for triggers, other than hydraulic ones, such as earthquakes, the degradation of the stability of these structures by internal erosion in the first two phases is more crucial.

There are several forms of internal erosion for the first two phases, among which suffusion is the focus in this study, since it progresses and puts structures in danger, while going unnoticed. Suffusion is internal erosion in which the seepage-induced loss of soil integrity occurs with the migration and loss of finer particles. Fannin and Slangen (2014) defined the difference using a similar form called suffosion. According to their definition, suffosion involves a reduction in volume during the seepage-induced erosion of finer particles, while suffusion does not. Typically, suffosion occurs when the fines content is large and the finer particles contribute to the formation of the soil skeleton. Since suffusion causes the migration and loss of finer particles without significant change in volume, it alters the soil state from dense to loose (Muir Wood et al., 2010), possibly leading to marked changes in the mechanical properties.

While many efforts have been made to understand the development of suffusion/suffosion at the element level or in a one-dimensional system, studies on the consequences of their occurrence on the mechanical properties of soil have been limited. Most of the studies have been performed on gap-graded soils that consist of binary granular mixtures, namely, soil mixtures containing coarser and finer particles with a large difference in their particle size distribution. Drained triaxial compression tests on eroded gap-graded soil (Chang and Zhang, 2011; Ke and Takahashi, 2014b, 2015) indicated that erosion made dilative soil contractive and that the strength of the soil decreased with erosion, as expected. Similar results were also obtained from drained torsional tests (Kuwano et al., 2021). As for undrained shearing tests on eroded gap-graded soil, conclusions differ depending on the researchers: (1) as expected, Prasomsri and Takahashi (2020, 2021) reported that erosion made the soil more contractive, that stiffness and strength decreased with erosion in triaxial compression tests, and that the cyclic resistance was smaller for eroded soil in cyclic triaxial tests, and (2) contrary to expectation, Xiao and Shwiyhat (2012), Ke and Takahashi (2014a), Ouyang and Takahashi (2016) Mehdizadeh et al. (2017a, 2017b, 2019), and Chitravel et al. (2023) reported that erosion made contractive soil dilative or less contractive, that stiffness and strength increased with erosion in triaxial compression tests, and that the cyclic resistance was larger for eroded soil in cyclic triaxial/torsional tests. Probably the latter results, those contrary to expectation, can be attributed to a coarser particle rearrangement accompanied by a reduction in volume due to erosion, i.e., the soils suffered from suffosion. As undrained shearing involves a decrease in effective stress, the differences in the initial soil fabric, i.e., the way in which the specimens are made, and the erosion-induced heterogeneity of the soil, can sensitively alter the soil's response during shearing, which may be another reason why these results contradict the undrained test results. In any case, as concrete conclusions have not been reached from the experimental studies on the mechanical properties of eroded soil, further elaboration is crucial.

Although there have been many experimental studies on backward erosion piping (Richards and Reddy, 2012; van Beek et al., 2015; Koito et al., 2016; Takizawa et al., 2018; Robbins et al., 2018; Vandenboer et al., 2018; Ovalle-Villamil and Sasanakul, 2021, 2022; Okamura et al., 2022; Pol et al., 2022; Peng et al., 2024 among the others), experimental studies on suffusion in earthen structures, based on physical model tests, are limited. The works by Horikoshi and Takahashi (2015a, 2015b) and Johnston et al. (2023) are exceptions, but their tests have certain limitations because of the small-scale models they used at the 1 g condition.

Moreover, as mentioned above, for proper earthquake-induced failure risk assessments of earthen structures that have suffered from repeated seepage, the seismic performance of earthen structures that have been deteriorated by suffusion should be studied. To the authors' knowledge, there have been no experimental studies reported in literature that deal with the seismic performance of earthen structures deteriorated by suffusion, although an experimental work dealing with a similar phenomenon in reverse order, i.e., the rainfall-induced failure of a slope deteriorated by an earthquake (Xu et al., 2022), does exist.

In the present study, employing a levee as an earthen structure, shake table tests are performed on the levee after causing its deterioration by seepage-induced suffusion in a geotechnical centrifuge to investigate the effects of suffusion-induced heterogeneity and mechanical characteristics change on the seismic response of the levee. In the tests, the model levee is subjected to repeated seepage flow in the geotechnical centrifuge to examine the progression of suffusion in the levee. Then, the effect of the suffusion-induced deterioration on the seismic response of the levee is subsequently examined by shake table tests on the geotechnical centrifuge (Takahashi et al., 2024).

2. Overview of centrifuge model tests

The centrifuge model tests are performed at 25 g on a Tokyo Tech Mark III centrifuge with a radius of 2.45 m (Takemura et al., 1999). The centrifugal acceleration for the tests is determined by the capacity of the water pump, which will be explained later. The model ground consists of a foundation ground and a levee. The model ground is prepared in a rigid aluminium container with inner dimensions of 600 × 250 × 400 mm in the model scale (25 × 6.25 × 10 m in the prototype scale.) The model ground and water circulation system in the prototype scale are shown in Fig. 1. All

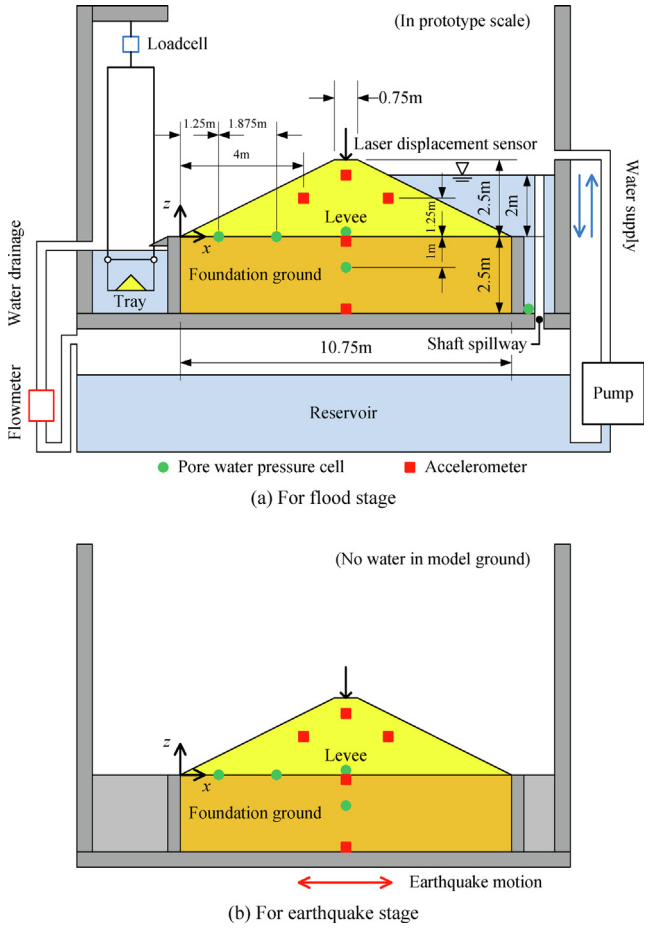

Fig. 1. Model setups in prototype scale.

the test conditions and results hereinafter are given in the prototype scale unless otherwise mentioned.

The inside of the model container is divided into three sections by retaining walls, namely, a water supply section modelling the flood channel on the right, a model section at the centre, and a water drainage section on the left protected side. The retaining walls form impermeable side boundaries. In the flood stage, to be explained later, water is pumped up from a reservoir under the model container and supplied to the flood channel on the right, as shown in Fig. 1a. The pump is a magnetic drive pump with a maximum discharge capacity of 40 L/min and a maximum lifting height of 14.3 m. Seepage tests are performed, while keeping the high water level constant, with the help of a shaft spillway in the flood channel on the right, and seepage is repeatedly initiated by raising and lowering the water level by turning the pump on and off. The rising rate of the water level is around 0.6 m/h, while the falling rate is around 0.7 m/h in the prototype scale. In actual situations, these rates are related to the capacity of rivers and cannot be generalised. According to the data collected by the Flood Disaster Prevention Division of the National Institute for Land and Infrastructure Management (2018), the majority of rising rates for small- to medium-sized rivers, whose watershed areas are less than 20 km^2, falls within a range of 0.5 to 1.5 m/h in Japan; and thus, the test conditions in this study are set within this range. In the earthquake stage, to be explained later, the retaining walls in the container are braced to minimise the vibrations and outward deformation of the walls during shaking, the water reservoir under the model container is removed, and the model container is directly mounted onto the shake table on the centrifuge, as shown in Fig. 1b.

To simplify the phenomenon, a mixture of fine and coarse fractions, namely, a gap-graded soil, is used for the model. Although gap-graded soil can cause an exaggeration of the test results, it allows for the (1) easy distinction between the base and the erodible materials and (2) easy observation of the fines migration in a short period. Based on the works by our research group (Ke and Takahashi, 2012, 2014a, 2014b, 2015; Horikoshi and Takahashi, 2015a, 2015b; Ouyang and Takahashi, 2016; Prasomsri and Takahashi, 2020, 2021), Silica Nos. 3 and 8 are chosen for use as the model materials. Silica No. 3 is used to model the soil skeleton, while Silica No. 8 is used to model the erodible fine particles in the voids of the coarse skeleton. Hereinafter, Silica No. 8 is referred to as fines for simplicity, even though Silica No. 8 is not strictly classified as fines by any soil classification standards based on its particle size. The initial fines content (percentage of mass ratio of Silica No. 8 to the total mass of the soil specimen, FC) of 25 % is selected, as the finer fraction offers a minor contribution to the coarser skeleton according to Prasomsri and Takahashi (2020). The physical and grading properties of the materials used in the study are summarised in Table 1. Susceptibility to the internal instability of the mixture is assessed based on the criteria of Kézdi (1979) and Kenney and Lau (1985, 1986). According to the parameters summarised in Table 1, the mixture is judged to be internally unstable.

The thickness of the model foundation ground is 2.5 m (100 mm in model scale) and the height of the levee with a

Table 1
Physical and grading properties of the materials.

Physical and grading properties	Silica No. 3	Silica No. 8	25 % Mixture
Specific gravity, G_s	2.645	2.645	2.645
Maximum void ratio, e_{max}	0.98	1.24	0.73
Minimum void ratio, e_{min}	0.75	0.88	0.44
Uniformity coefficient, C_u	1.47	2.18	11.41
Curvature coefficient, C_c	1.60	0.98	5.35
D_{15c} (mm)[a]	1.65	–	1.65
D_{85f} (mm)[a]	–	0.25	0.25
$(H/F)_{min}$[b]	–	–	0.62
Particle description	Sub-angular ~ Angular		

[a] D_{15c} is the particle diameter in which 15 % by mass of the coarse particles passed. D_{85f} is the particle diameter in which 85 % by mass of the fine particles passed. When $D_{15c}/D_{85f} \geq 4$, the soil is internally unstable (Kézdi 1979).

[b] F is the passed fraction by mass finer than d, and H is the mass fraction between d and $4d$. When $(H/F)_{min} \leq 1$, the soil is internally unstable (Kenney and Lau 1985, 1986).

slope of 1V:2H is the same as the thickness of the foundation ground. The relative density of the foundation ground is set at 60 %, while that of the levee is set at 50 %. These densities are relatively small compared to those of usual levees. They are determined by the test conditions for laboratory works on gap-graded soil by our research group, as mentioned above. For the foundation ground, yellow Silica No. 8 is used for the fines, while blue Silica No. 8 is used for the levee. The soil is compacted to form the foundation ground and levee with a water content of 5 %. Firstly, the foundation ground is prepared by placing and compacting the mixture in five layers. Each layer is compacted to have an equal thickness of 0.5 m with the target density. Then, the levee layer is prepared by placing and compacting the mixture in four layers (thicknesses of 0.5, 0.75, 0.75 and 0.5 m from the bottom) using temporary supports. While preparing the model ground, miniature pore water pressure cells (maximum measurable pressure = 20 0 kPa) and piezoelectric accelerometers are placed in the predetermined locations shown in Fig. 1. Finally, the model levee layer is cut to the designed configuration by the placing of a template having the same dimensions as the levee. After completing the model preparation under a partially saturated condition, the model foundation ground is saturated with water at 1 g. At this stage, the apparent water level in the model is higher than the top of the foundation ground. The laser displacement sensors, flowmeter (maximum measurable flow rate = 10 L/min), and eroded soil measurement tray with a loadcell (maximum measurable load = 100 N) are also placed in predetermined locations before the tests.

One test consists of two stages, namely, the flood stage and the earthquake stage. In the flood stage, firstly, the centrifuge is spun up to 25 g and a steady state is ensured by allowing the pore water pressure measurement to stabilise. At this stage, the water level in the model is at the top of the foundation ground and the levee is almost dry. The repeated flooding of a river channel is then simulated by raising and lowering the water level on the flood channel side by turning the pump on and off. The scaling in time for the flood stage is made with a commonly used scaling factor for the centrifuge tests, i.e., the seepage time in the prototype scale is 25^2 times that in the model scale. Thus, the flow velocity in the soil in the prototype scale is 1/25 times that in the model scale. This means that the hydraulic conductivity in the prototype becomes 1/25 times that in the model scale when the hydraulic gradient is defined using the water head based on the dimensions. Fig. 2 plots the time history of the flood water level for the case with 12 cycles of repeated seepage. The high water condition (a water level at 80 % of the levee height) is maintained for around 100 h (around 10 min in model scale) for each flood cycle. For easy comparison, all the time evolutions in the following are plotted against the cumulative seepage time by omitting the time for the non-high-water levels as in the plot at the bottom of Fig. 2. This kind of treatment is possible since (1) the seepage flow in the embankment

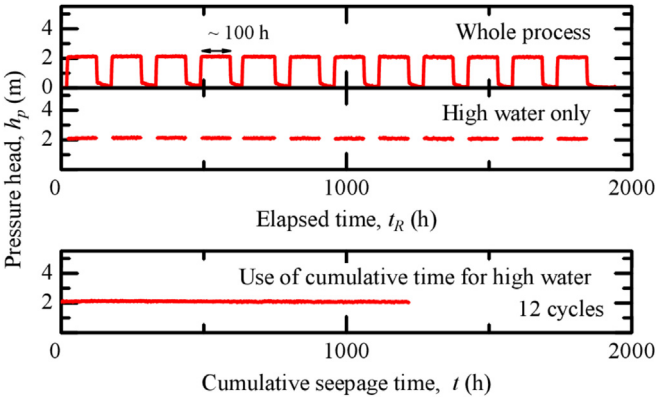

Fig. 2. Time history of flood water level and explanation of cumulative seepage time.

almost instantaneously reached a steady state once the water level on the flood channel side reached the high water level and (2) all the sensor readings returned to the same value after a cycle of lowering and raising the flood water level. The former is due to the relatively large hydraulic conductivity of the soil and the high degree of saturation of the soil below the phreatic surface. In the experiment, (1) to examine the progression of suffusion from the fines content distributions after the tests, and (2) to create a levee suffered from different levels of suffusion, tests having the same initial conditions, but a different number of repeated seepage flows, are performed (no seepage, 6, 12 and 20 cycles of seepage). The test conditions are summarised in Table 2. After applying the repeated seepage, the centrifuge is spun down to 1 g. The eroded soil is collected and the necessary measurements are made at 1 g. The water level in the model ground is then lowered to the bottom of the foundation ground for the next earthquake stage. The reason for making the model ground dry in the earthquake stage is that a saturated foundation ground will cause the large deformation of the levee due to liquefaction, and this will make it difficult to evaluate the impact of the suffusion-induced deterioration of the soil on the dynamic response of the levee.

In the earthquake stage, firstly, the centrifuge is spun up to 25 g, and the water is fully drained out by opening the drain at the bottom of the container in the model ground and allowing some time. Then, the three earthquake motions shown in Fig. 3 are applied to the model ground under dry conditions. The input earthquake motions are essentially sinusoidal waves with a frequency of 2 Hz (50 Hz in model scale.) As the asymmetric dynamic response of the levee is expected, due to the asymmetric levee deterioration by the seepage flow, symmetric earthquake motions are selected. As for the motion in Step 1, since the shake table was not controlled well, the earthquake motion had a wide range of frequency components. Thus, the response of the model in Step 1 is later used to obtain the transfer function of the levee and to estimate the natural frequency of the levee. The scaling in time for

Table 2
Test conditions and some results (all values are in prototype scale).

Test code	No seepage	6 cycles	12 cycles	20 cycles	Continuous
Initial fines content, *FC*	25 %	25 %	25 %	25 %	25 %
Initial soil mass ratio passing 425 μm sieve, *FC′*	25.7 %	25.7 %	25.7 %	25.7 %	25.7 %
Relative density of levee	50 %	50 %	50 %	50 %	50 %
Relative density of foundation ground	60 %	60 %	60 %	60 %	60 %
Number of seepage cycles, *N*	0	6	12	20	1
Total seepage time (h)	0	605	1220	2000	1240
Initial pressure head at flood channel (m)	–	2.05	2.10	2.09	2.07
Initial flow rate, q_0 (m^3/m/s)	–	2.0×10^{-4}	1.8×10^{-4}	1.5×10^{-4}	1.5×10^{-4}
Total eroded soil mass, m_e (kg/m)	0	23.4	38.0	39.6	36.2
Crown settlement in Step 3 (m)	0.25	0.27	0.28	0.29	–

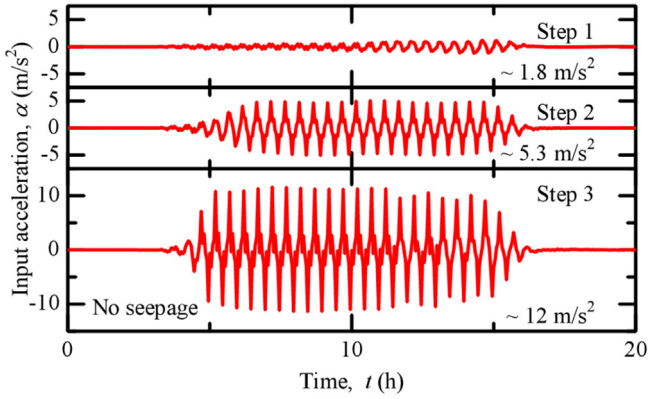

Fig. 3. Input earthquake motions (No seepage).

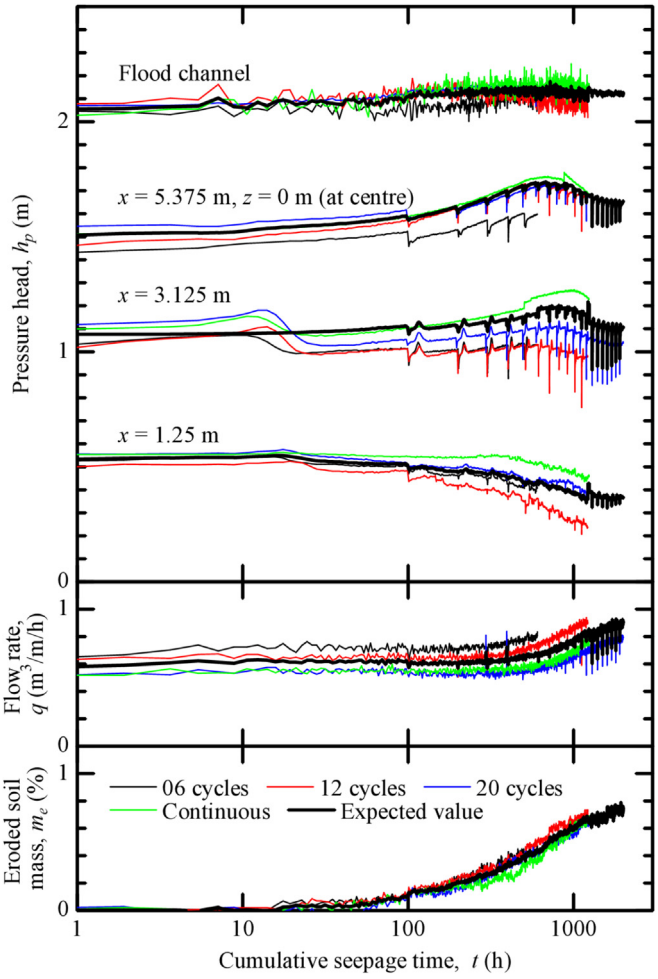

Fig. 4. Time evolution of pressure head, flow rate, and eroded soil mass.

the earthquake stage is made using a commonly employed scaling factor for the centrifuge tests, i.e., the time in the prototype scale is 25 times that in the model scale. After applying the earthquake motions, the centrifuge is spun down to 1 g. The necessary measurements are made at 1 g, and sieve tests are performed to examine the distribution of the fines content in the model ground. The fines content is estimated with a 425-μm sieve. However, since a small amount of particles passing through the 425 μm sieve exists in Silica No. 3, this should be considered when estimating the changes in the fines content by this sieve test. As the ratio of the initial soil mass passing through the 425-μm sieve is 25.7 %, this value is used to estimate the suffusion-induced change in the fines content.

3. Responses of levee in flood stage

3.1. Changes in pressure head, flow rate, and eroded soil mass

Fig. 4 shows the time evolutions of the pressure head, flow rate, and eroded soil mass for all the cases with the expected values. Here, the cumulative seepage time is the elapsed time, excluding the time the water supply is stopped, as previously demonstrated in Fig. 2. The pressure head is estimated by the readings of the pore water pressure cells placed on top of the foundation ground (see Fig. 1) and at the bottom of the water supply section by setting the base at the top of the foundation ground. The normalised cumulative eroded soil mass is the discharged soil mass normalised by the fine particles existing below the initial phreatic surface. The initial pressure head at the flood channel, initial flow rate, and total eroded soil mass for each case are provided in Table 2. As for the expected values, they are estimated by averaging the available measurements at the same time, in principle, except for the pressure head at $x = 3.125$ m, in which a correction is made by

omitting the sudden change in the readings around the cumulative seepage time of 10 h.

Tests having the same initial conditions, but a different number of repeated seepage flows, are performed to examine the suffusion progression from the fines content distributions after the tests. Thus, all the sensor readings are expected to show the same time evolutions, but some variations exist due to several uncertainties in the model ground. The relatively smaller initial pressure head at the flood channel and larger initial flow rate in the cases with 6 and 12 cycles of repeated seepage suggest that the overall hydraulic conductivity of the levee in these cases is relatively large. They result in smaller pressure head readings in the levee and a larger eroded soil mass. As for the case with continuous seepage, the time changes in the pressure head near the toe ($x = 1.25$ m) and at the middle of the slope ($x = 3.125$ m) on the protected side are relatively small compared to the other repeated seepage cases. However, as these values are within the range of the variation, it can be said that the difference between the repeated and the continuous seepage flows is not very significant, at least for the pressure readings. Based on these findings, it can be said that the overall tendencies are all similar, as seen in the figure, indicating the repeatability/consistency of the tests. Regarding the levee settlement, there is almost no settlement during the repeated seepage, although the test data is not explicitly presented here. Thus, it can be said that the internal erosion occurring in this series of tests is suffusion, i.e., the seepage-induced erosion of finer particles without significant reduction in the volume of the soil.

Paying attention to the general trends in the time evolutions, the following points can be observed: (1) the eroded soil mass monotonically increases with time, (2) the pressure head monotonically decreases with time near the toe on the protected side ($x = 1.25$ m), while a trend to increase and then decrease can be seen below the crown ($x = 5.375$ m) and at the middle of the slope on the protected side ($x = 3.125$ m), (3) the flow rate increases along with a decreasing trend of the pressure head below the crown and at the middle of the slope on the protected side, and (4) all the readings cease to change after around 1500 h (15 cycles). These significant changes indicate that the change in the void ratio distribution caused by the migration of the fines occurs inside the embankment. To evaluate this, a simple estimation of the change in hydraulic conductivity will be made later to understand the state change in the levee.

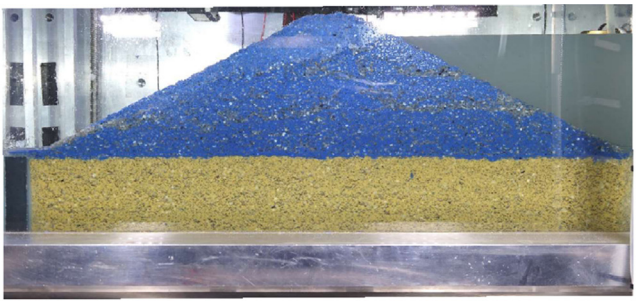

(a) During seepage (12 cycles)

(b) After seepage (12 cycles, top view near the toe)

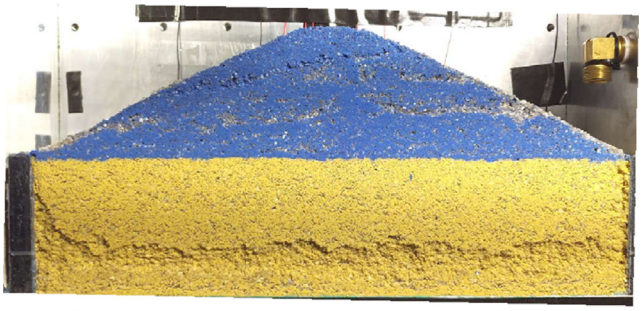

(c) After the test (12 cycles, near the window)

(d) After the test (12 cycles, at centre)

Fig. 5. Side and top views of model ground during and after the test (12 cycles).

3.2. Distribution of fines content after seepage

The side and top views of the model ground during seepage and after the test for the case with 12 cycles of repeated seepage are shown in Fig. 5. While the picture during seepage (Fig. 5a) is taken through the transparent window in front, those after the test (Fig. 5c and d) are taken after the removal of the transparent window. The top view of the toe on the protected side (Fig. 5b) is taken after the seepage test (before the shake table tests). Since the pictures in Fig. 5c and d are taken after the shake table tests, the levee shows some deformation. As the coarse particles of Silica No. 3 are pale and the fines are coloured, the pictures allow the visual confirmation of the distributions of fines. Near the window (Fig. 5a and c), some traces of the preferential horizontal flow and fines loss near the phreatic surface can be seen, while no such concentration can be seen at

the centre section (Fig. 5d). The former is due to the relatively larger void at the boundary with the rigid and flat walls parallel to the flow direction, as is typically seen in rigid wall permeameter tests. Although the top view of the toe on the protected side (Fig. 5b) suggests a somewhat larger amount of erosion near the walls parallel to the seepage direction, it can be said that it is not very significant and that erosion occurs rather in a two-dimensional manner.

The distributions of the fines content change for the cases with 6, 12 and 20 cycles of repeated seepage are shown in Fig. 6. The whole model ground is divided into 60 zones, and the sieving samples from all the zones determine the distributions of the changes in the fines contents. The negative values indicate a decrease in the fines content due to seepage. Since the large decrease in the zones near the toes is affected by the great loss in fines at the surface, i.e., in the very shallow portion of the slope, seen as the pale cover over the surface in Fig. 5c and d, care is required when interpreting these findings. Even if these zones are ignored, a significant decrease is observed near the toe on the left protected side and some increase in the foundation ground after six cycles of repeated seepage (Fig. 6a). With further seepage cycles, the fines content is seen to also decrease in the middle part of the levee and foundation ground (Fig. 6b and c). In all the cases, a loss of fines is also observed near the toe on the right flood channel side probably due to the rightward seepage during the drawdown of the flood water. The vertical movement of fines can also be confirmed by the interfusion of blue particles (fines originated in the levee) to the foundation ground in Fig. 5. These indicate that the eroded fines move laterally by advection due to seepage flow and vertically due to the gravitational force resulting in deposition in the foundation ground, which is consistent with the observation by Horikoshi and Takahashi (2015a, 2015b), even though the boundary conditions and stress levels are different. A clearer and obvious time change in the fines content distribution was expected. Unfortunately, it was not realised because of the small change in fines content and the variation caused by the small volume of samples used for the sieve tests. Since significant changes can be observed in the mechanical and hydraulic characteristics of the gap-graded soil by the small amount of fines loss induced by seepage (even less than 1 %) in the laboratory tests, e.g., Prasomsri and Takahashi (2020, 2021), it can be said that the changes in the fines content in the tests are at a significant level. As indicated in the previous subsection, notable changes in the pore water pressure and the evolution of the eroded soil mass are evidence of the changes in the void ratio distribution induced by the migration of fines in the core part of the levee, which will be explored in the next section through a simple estimation.

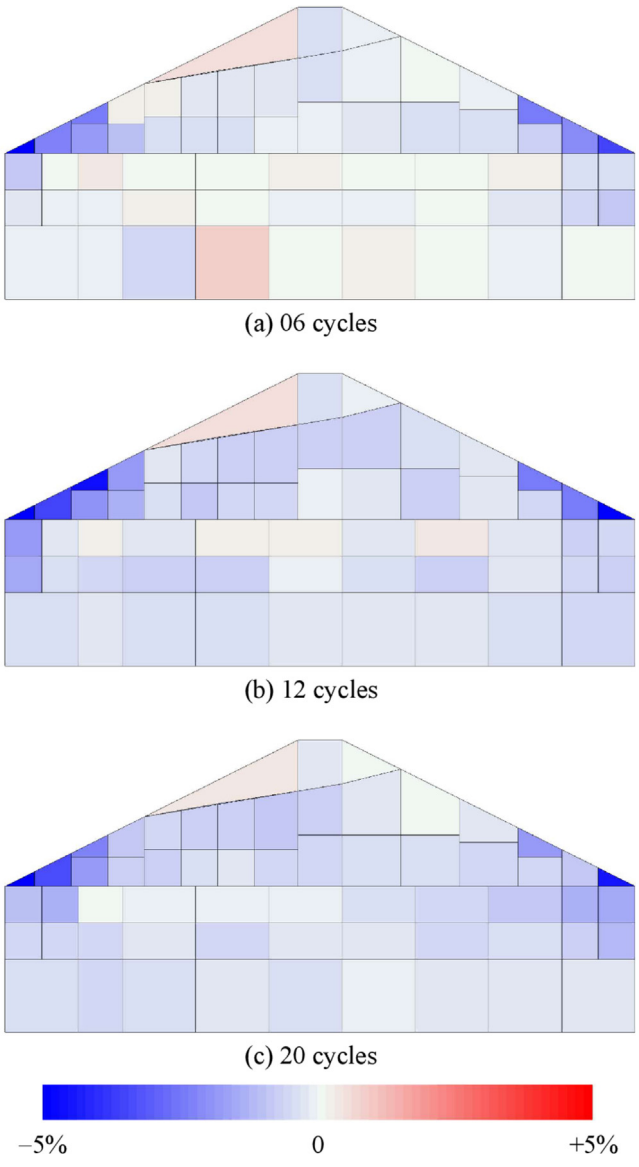

Fig. 6. Distributions of changes in fines content $\Delta FC'$ (6, 12 and 20 cycles).

4. Estimation of suffusion-induced changes in hydraulic conductivity and fines content

An attempt is made to estimate the change in hydraulic conductivity based on Dupuit's assumption for a nearly horizontal unconfined flow using the measured water heads and discharge. With the help of the Kozeny-Carman equation (Carman, 1937) or the equivalent equation proposed by Taylor (1948) for the estimation of the hydraulic conductivity of soil considering various factors, the change in the void ratio due to suffusion in the levee is estimated and converted to the change in the fines content.

In the application of Dupuit's assumption for the flow in a levee, (1) it firstly has to be confirmed that the seepage flow in the levee is nearly horizontal and (2) the proportion of water seeping through the levee has to be estimated since the target model levee is a two-layer system, i.e., the flow in the lower layer can be modelled as a horizontal confined flow without the exchange of water from the upper layer.

To confirm these, a simple two-dimensional steady-state seepage analysis is performed. Taylor's equation for hydraulic conductivity is expressed as

$$k = D_s^2 \frac{\gamma_w}{\mu}\left(\frac{e^3}{1+e}\right)C \propto \left(\frac{e^3}{1+e}\right) \quad (1)$$

where k = hydraulic conductivity, D_s = effective particle size, γ_w = unit weight of water, μ = viscosity of water, e = void ratio, and C = composite shape factor. Assuming that none of the parameters, except for the void ratio, change due to suffusion or a small difference in the soil density, the hydraulic conductivity is proportional to $\left(\frac{e^3}{1+e}\right)$. If this applies to the material used in the tests, the initial hydraulic conductivity of the foundation ground is 0.8 times that of the levee. Two-dimensional steady-state seepage analysis results under this condition are shown in Fig. 7. The hydraulic boundary conditions for the analysis are the same as those in the experiment. To model the partially saturated soil, the van Genuchten model with the Mualem model (van Genuchten 1980) is used. The material parameters applied here are summarised in Table 3. The seepage flow direction is almost horizontal under the protected side slope, and it is found that the proportion of water seeping through the levee is around 40 % of the total flow. Thus, it is decided that the flow in the levee is modelled based on Dupuit's assumption. The flow rate in the levee is assumed to be 40 % of the expected total flow rate in Fig. 4 to estimate the changes in the hydraulic conductivity in the levee. In the tests, a change in the fines content, i.e., hydraulic conductivity, in the foundation ground is also expected. This may alter the proportion of water seeping through the levee with time, but the proportion is kept constant for simplicity.

Since the number of measurement points for the pore water pressure is limited, the levee is divided into three areas, as shown in Fig. 8, and estimations of the hydraulic conductivity are made for these areas. The coordinates used in Fig. 8 are the same as those in Fig. 1. The location of the upstream boundary of Area 0 is determined by the classic approximating method by Casagrande (1940), and

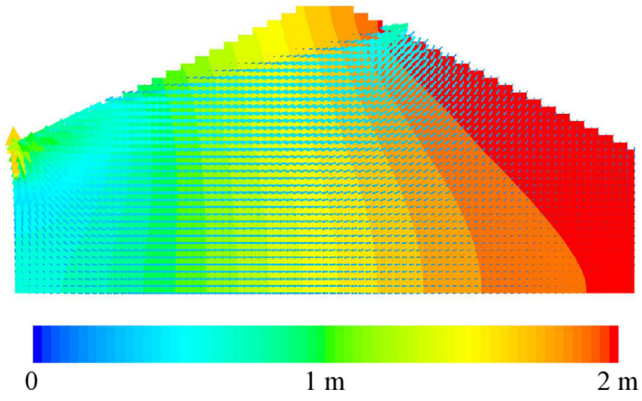

Fig. 7. Water head distribution and flow vectors in two-dimensional seepage analysis.

Table 3
Parameters used in seepage analysis.

Parameter	Value
Saturated hydraulic conductivity for foundation (m/s)	1.9×10^{-4}
Saturated hydraulic conductivity for levee (m/s)	2.3×10^{-4}
α for van Genuchten model (1/m)[a]	57.9
n for van Genuchten model[a]	1.62
m for van Genuchten model[a]	$1 - 1/n$

[a] Based on the parameters determined by Horikoshi and Takahashi (2015b).

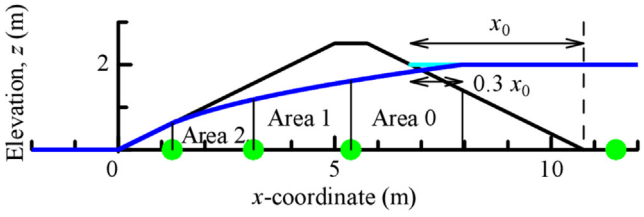

Fig. 8. Division of levee for estimation of changes in hydraulic conductivity and fines content.

the water level at this location is assumed to be the same as the value in the flood channel. Based on Dupuit's assumption, the hydraulic conductivity of an area can be estimated by

$$k = \frac{2Lq}{\left(H_u{}^2 - H_d{}^2\right)} \quad (2)$$

where L = length of the area in the flow direction, q = flow rate per unit width, and H_u, H_d = water levels at the upstream and downstream boundaries of the area.

Since no significant settlement of the levee occurs during seepage, i.e., suffusion occurs as mentioned in Section 3.1, the change in the fines content is estimated by assuming no volume change in the soils. Assuming that none of the parameters, except for the void ratio in Eq. (1), change due to suffusion, the change in the fines content can be estimated by the following relationship:

$$e = e_0 - (1 + e_0)\Delta FC \quad (3)$$

where e = current void ratio, e_0 = initial void ratio, and ΔFC = change in the fines content (negative in fines loss) when the specific gravities of the coarse particles and the fines are the same.

Fig. 9 plots the time evolutions of the estimated hydraulic conductivity and the fines content using the expected values in Fig. 4. The changes in the measured fines content are also plotted in the figure. The measured value is calculated by the weighted averaging of the changes in the fines content in the corresponding area. As for the estimated hydraulic conductivity, the values in Areas 1 and 2 are very similar at the beginning, while that in Area 0 is smaller than the others. This is because the flow in Area 0 is not that in Dupuit's assumption. Apart from this, the evolutions of the estimated hydraulic conductivity and the changes in the fines content appear to be exaggerated, although

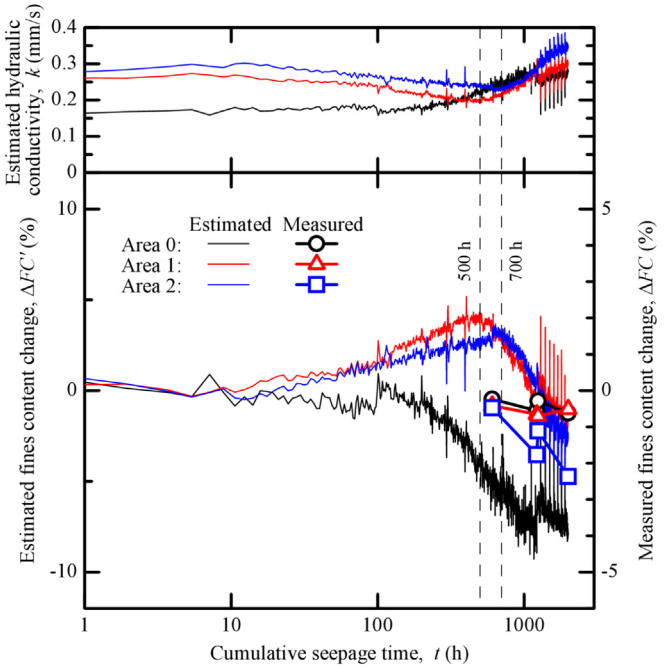

Fig. 9. Time evolutions of estimated hydraulic conductivity and changes in fines content.

reasonable, since the changes in the fines content in each area show a decreasing trend earlier in the area closer to the flood channel side; the decrease starts from the beginning in Area 0, around $t = 500$ h (5th seepage cycle) in Area 1, and around $t = 700$ h (7th seepage cycle) in Area 2. The increase before the decrease in Areas 1 and 2 is due to the advection of fines toward the protected side. Although the values are not estimated in the area left of Area 2 (at the toe on the protected side), according to the pressure head near the toe on the protected side ($x = 1.25$ m) in Fig. 4, the hydraulic conductivity and fines content are expected to change similarly, but greatly, compared to Area 0.

It is inferred that, due to the advection of fines toward the protected side, the changes in the fines content tend to reach a steady state gradually from the flood channel side, and this area expands toward the protected side, except near the toes. As the estimated changes in the fines content are not the same, but show trends similar to the measured ones, it can be said that, even with such a simple calculation, the progression of suffusion is schematically explicable.

5. Seismic response of levee in earthquake stage

5.1. Changes in shear wave velocity/stiffness with erosion

The effect of the suffusion-induced deterioration on the seismic response of the levee is subsequently examined by shake table tests. In the flood stage, seepage-induced suffusion, i.e., fines loss without a change in soil volume, made the void ratio larger. This can be viewed as soil loosening due to the loss of fines, leading to decreases in the unit mass (ρ) and shear modulus (G). The shear modulus and shear wave velocity (V_s) are related in the form of $G = \rho V_s^2$. By analogy with the fact that the natural period in the fundamental mode (T_1) for the uniform and horizontally layered deposit, whose thickness $= H$, is $T_1 = 4H/V_s$, it can be said that the natural frequency (inverse number of the natural period) of the levee and shear wave velocity of the soil in the levee are good indices for examining the suffusion-induced loosening or deterioration of the soil. Thus, the propagation of the wave in the levee is examined first, as the foundation ground is confined by rigid retaining walls in this series of tests.

The transfer functions that determine the frequency-dependent amplification through the levee are estimated from the acceleration records at the boundary between the levee and the foundation ground and just below the levee crown in Step 1, and are plotted in Fig. 10. The natural frequency of the levee can be estimated from the frequency for the peak in the transfer function. The natural frequency is expected to be smaller for the deteriorated levee. A decrease in natural frequency, compared to the no seepage case, is significant in the cases whose seepage cycles are 12 and 20. As explained in Figs. 6 and 9, because the decrease in fines in the middle of the levee is not very significant in the case with 6 seepage cycles, the natural frequency for this case is comparable to the case without seepage.

For Steps 2 and 3 with larger shaking, the equivalent shear wave velocity in the levee is estimated by the travel time between the two measurement points mentioned above. The equivalent shear wave velocity is plotted against the number of seepage cycles in Fig. 11. For comparison, the shear wave velocity in Step 1 is estimated using an equivalent single degree of freedom model for the embankment (Sakai et al., 2017), and is also plotted in the figure. Due to the large earthquake motions in Steps 2 and 3, the estimated shear wave velocity is affected by the plastic deformation of the levee, resulting in a much smaller velocity. In all the shaking steps, the shear wave velocity decreases with the number of seepage cycles, indi-

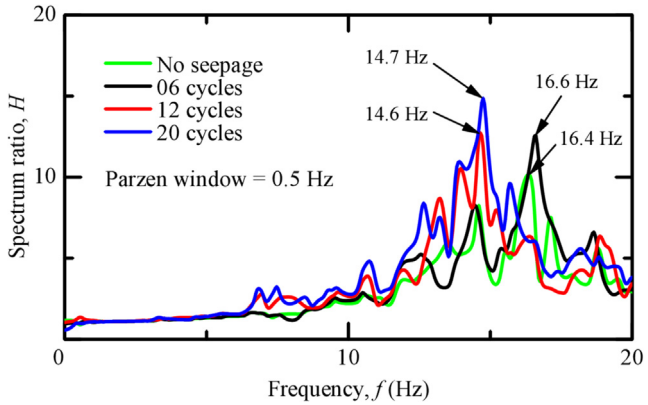

Fig. 10. Transfer functions for levee in Step 1.

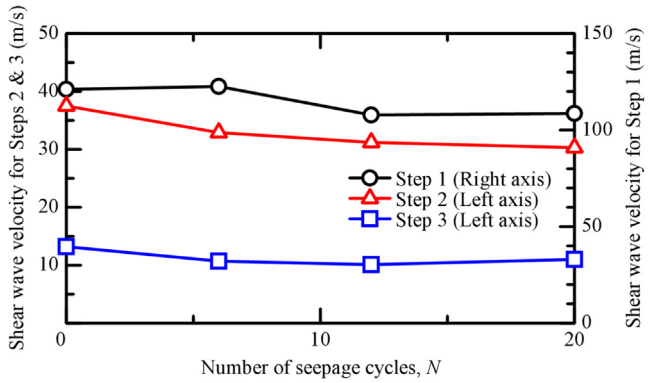

Fig. 11. Changes in equivalent shear wave velocity with number of seepage cycles.

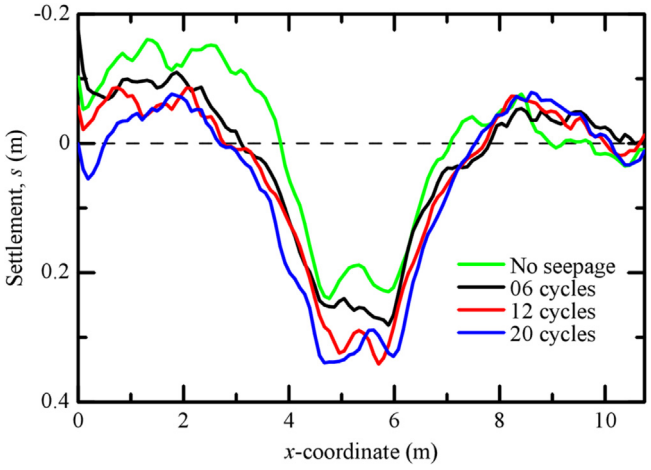

Fig. 13. Distributions of levee surface settlement after the test.

cating a decrease in stiffness due to the suffusion with a large number of seepage cycles or a longer seepage period.

5.2. Changes in strength and cyclic-shearing-induced compression with erosion

The side views of the model ground before and after shakings, for the case with 20 cycles of repeated seepage, are shown in Fig. 12. Distributions of the levee surface settlement estimated by the measurements before and after the test at the centre line are plotted in Fig. 13. The latter is measured by a depth camera (Intel RealSense LiDAR Camera L515) at 1 g. Ito et al. (2021) used a similar sensor to measure the change in temporal topography due to the backward erosion piping during the spinning of the centrifuge. However, in this study, the measurements are made at 1 g before and after each centrifuge test. In this series of tests, no earthquake-induced levee failure occurs and no clear slip surface appears. Instead, marked settlement with the bulging of the levee is observed in all the cases, as shown in the figures. The settlement at the crown is seen to be relatively larger for the case with the larger number of seepage cycles.

Fig. 14 plots the time histories of the crown settlement in Steps 2 and 3. Although the case with the larger number of seepage cycles shows a relatively larger settlement, the difference is minor, suggesting no marked change in strength or cyclic-shearing-induced compression. Wang et al. (2021) summarised shearing tests on internally eroded gap-graded soil and indicated that the angle of shearing resistance decreases with the loss in fines content. However, in this series of tests, the seepage-induced loss of fines is notice-

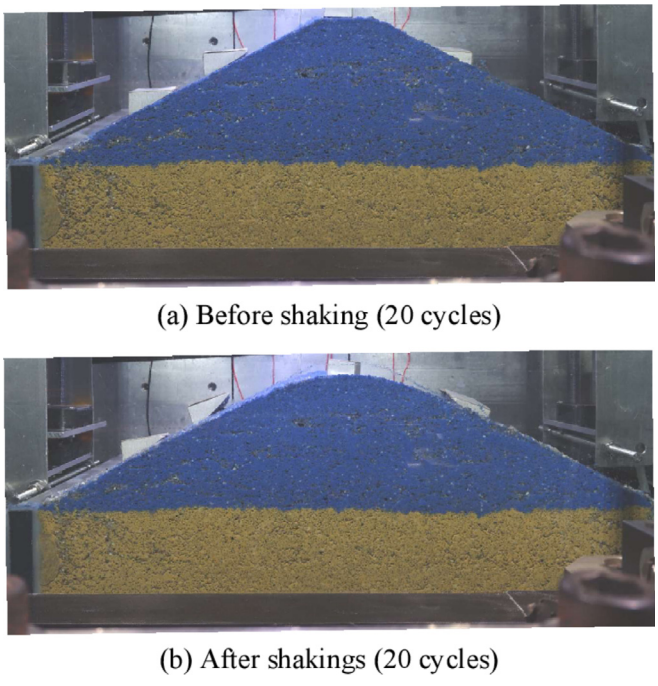

Fig. 12. Side views of model ground before and after shakings (20 cycles).

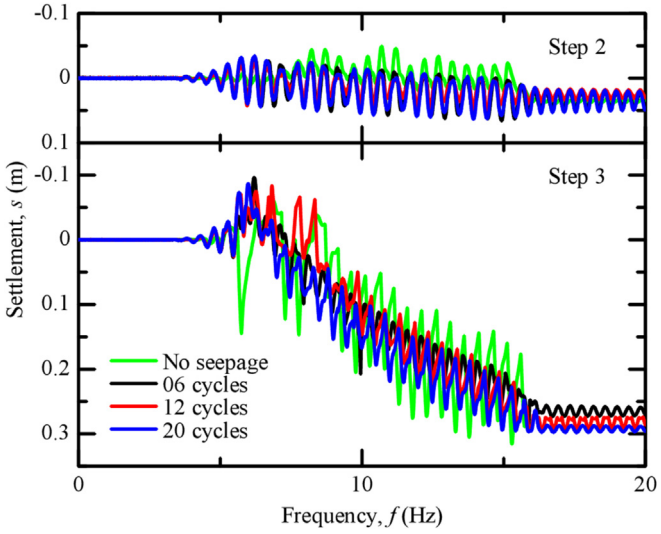

Fig. 14. Time histories of the crown settlement in Steps 2 and 3.

able. but not large, suggesting that the change in erosion-induced strength is minor. They also reported that the shearing-induced volume change characteristics do not change much by suffusion. For these reasons, there is no significant difference in the levee settlement based on the seepage cycles or seepage period within the scope of the present study.

6. Conclusions

In this study, shake table tests on a levee deteriorated by seepage-induced internal erosion are performed in a geotechnical centrifuge at 25 g to investigate the effects of erosion-induced heterogeneity and mechanical characteristics change on the seismic response of the levee. Among the several forms of internal erosion, suffusion, in which the seepage-induced loss of soil integrity occurs with the migration and loss of finer particles, is the focus of this study, since it progresses and puts structures in danger, while going unnoticed. The target structure is a 2.5-m levee built on a 2.5-m-thick foundation ground. One test consists of two stages: the flood stage and the earthquake stage. The model ground made of gap-graded soil, with a fines content of 25 %, is firstly subjected to repeated seepage flow by changing the water level in the flood channel. The high water level is at 80 % of the levee height, and is maintained for around 100 h for each flood in the prototype scale. After lowering the water level, earthquake motions are applied to the dried model deteriorated by suffusion. In the flood stage, (1) to examine the suffusion progression from the fines content distributions after the tests, and (2) to create a levee suffered from different levels of suffusion, a different number of repeated seepage flows is applied for each case. The major findings obtained in this study are as follows:

- A significant decrease in the fines content is observed near the toe on the protected side and some increase is observed in the foundation ground due to the flood-induced seepage flow after six cycles of repeated seepage (corresponding to the cumulative seepage time of 600 h). With further seepage cycles, the fines content decreases in both the levee and the foundation ground. These findings indicate that the eroded fines move laterally by advection due to the seepage flow and vertically due to the gravitational force, resulting in deposition in the foundation ground.
- The changes in hydraulic conductivity, void ratio, and fines content due to suffusion under the seepage flow are estimated from the changes in the pressure heads at the base of the levee and the discharge by a simple calculation based on Dupuit's assumption and the Kozeny-Carman equation or equivalent. These estimations are helpful for understanding the advection of fine particles with the progress of suffusion. From the estimated changes in the fines content, it is inferred that the seepage-induced transport of fines tends to reach a steady state gradually from the flood channel side and that the area expands toward the protected side, except near the toes.
- Changes in suffusion-induced soil stiffness are confirmed by a significant decrease in the natural frequency of the levee and the equivalent shear wave velocity in the levee in cases where the number of seepage cycles is larger.
- In this series of tests, no earthquake-induced levee failure occurs and no clear slip surface appears. Instead, marked settlement with bulging of the levee is observed. Although the case with the larger number of seepage cycles shows a relatively larger earthquake-induced settlement, the difference is minor, suggesting that no marked change in strength or compression due to cyclic shearing within the scope of this study.

CRediT authorship contribution statement

Akihiro Takahashi: Writing – original draft, Visualization, Supervision, Methodology, Funding acquisition, Formal analysis, Conceptualization. **Tamaki Inoue:** Writing – review & editing, Visualization, Investigation, Formal analysis. **Saki Yamagata:** Writing – review & editing, Visualization, Investigation, Formal analysis. **Kazuki Horikoshi:** Writing – review & editing, Visualization, Methodology.

Acknowledgements

This work was supported by JSPS KAKENHI Grant Nos. 19H02232 and 23K26193. The authors are indebted to Mr Sakae Seki, a technician at the Institute of Science Tokyo, for his continued cooperation with the centrifuge experiments.

References

Carman, P.C., 1937. Fluid flow through granular beds. Trans. Inst. Chem. Eng. 15, 150–166. https://doi.org/10.1016/S0263-8762(97)80003-2.

Casagrande, A., 1940. Seepage through Dams. Contributions to Soil Mechanics. Boston Society of Civil Engineers, Boston, pp. 1925–1940.

Chang, D.S., Zhang, L.M., 2011. A stress-controlled erosion apparatus for studying internal erosion in soils. *Geotech. Test. J.* 34 (6), 579–589. https://doi.org/10.1520/GTJ103889.

Chitravel, S., Otsubo, M., Kuwano, R., 2023. Effects of seepage flow on liquefaction resistance of uniform sand and gap-graded soil under undrained cyclic torsional shear. *Soils Found.*, 63 (5). https://doi.org/10.1016/j.sandf.2023.101363 101363.

Fannin, R.J., Slangen, P., 2014. On the distinct phenomena of suffusion and suffosion. *Géotechnique Lett.* 4 (4), 289–294. https://doi.org/10.1680/geolett.14.00051.

Flood Disaster Prevention Division of National Institute for Land and Infrastructure Management, 2018. Guideline for Estimating Flood Water Level Rising Rate in Small and Medium Size Rivers without Water Level Monitoring Data (in Japanese) https://www.nilim.go.jp/lab/rcg/newhp/seika.files/pdf/tebiki_1-2.pdf [Accessed 30 Nov 2024].

Foster, M., Fell, R., 1999. A framework for estimating the probability of failure of embankment dams by internal erosion and piping using event tree methods UNICIV Report No. 377. University of New South Wales, Sydney, Australia https://vm.civeng.unsw.edu.au/uniciv/R-377.pdf.

Horikoshi, K., Takahashi, A., 2015a. Suffusion-induced change in spatial distribution of fine fractions in embankment subjected to seepage flow. *Soils Found.* 55 (5), 1293–1304. https://doi.org/10.1016/j.sandf.2015.09.027.

Horikoshi, K., Takahashi, A., 2015b. Effects of redeposition of fines on seepage-induced fines transport in embankments. *Jpn. Geotech. J.* 10 (4), 473–488. https://doi.org/10.3208/jgs.10.473 (in Japanese).

Ito, Y., Noda, S., Takahashi, A., Horikoshi, K., 2021. Measurement techniques for capturing piping-induced deformation of levees in centrifuge model. Proc. 10th Int. Conf. Scour Erosion, pp. 923–930 https://www.issmge.org/publications/publication/measurement-techniques-for-capturing-piping-induced-deformation-of-levees-in-centrifuge-model.

Johnston, I., Murphy, W., Holden, J., 2023. Alteration of soil structure following seepage-induced internal erosion in model infrastructure embankments. *Transp. Geotech.* 42. https://doi.org/10.1016/j.trgeo.2023.101111 101111.

Ke, L., Takahashi, A., 2012. Strength reduction of cohesionless soil due to internal erosion induced by one-dimensional upward seepage flow. *Soils Found.* 52 (4), 698–711. https://doi.org/10.1016/j.sandf.2012.07.010.

Ke, L., Takahashi, A., 2014a. Triaxial erosion test for evaluation of mechanical consequences of internal erosion. *Geotech. Test. J.* 37 (2), 347–364. https://doi.org/10.1520/GTJ20130049.

Ke, L., Takahashi, A., 2014b. Experimental investigations on suffusion characteristics and its mechanical consequences on saturated cohesionless soil. *Soils Found.* 54 (4), 713–730. https://doi.org/10.1016/j.sandf.2014.06.024.

Ke, L., Takahashi, A., 2015. Drained monotonic responses of suffusional cohesionless soils. *J. Geotech. Geoenviron. Eng.* 141 (8). https://doi.org/10.1061/(ASCE)GT.1943-5606.0001327 04015033.

Kenney, T.C., Lau, D., 1985. Internal stability of granular filters. *Can. Geotech. J.* 22 (2), 215–225. https://doi.org/10.1139/t85-029.

Kenney, T.C., Lau, D., 1986. Internal stability of granular filters: Reply. *Can. Geotech. J.* 23 (3), 420–423. https://doi.org/10.1139/t86-068.

Kézdi, A., 1979. Soil Physics: Selected Topics. Developments in Geotechnical Engineering. Elsevier Scientific Publishing Co., Amsterdam, p. 25, ISBN-13: 978-0444997906.

Koito, N., Horikoshi, K., Takahashi, A., 2016. Physical modelling of backward erosion piping in foundation beneath levee. In: Harris, J., Whitehouse, R., Moxon, S. (Eds.), Scour and Erosion: Proceedings of the 8th International Conference on Scour and Erosion (Oxford, UK, 12–15 September 2016). CRC Press, pp. 445–451. https://doi.org/10.1201/9781315375045.

Kuwano, R., Santa Spitia, L.F., Bedja, M., Otsubo, M., 2021. Change in mechanical behaviour of gap-graded soil subjected to internal erosion observed in triaxial compression and torsional shear. *Geomech. Energy Environ.* 27. https://doi.org/10.1016/j.gete.2020.100197 100197.

Mehdizadeh, A., Disfani, M.M., Evans, R., Arulrajah, A., Ong, D.E.L., 2017a. Mechanical consequences of suffusion on undrained behaviour of a gap-graded cohesionless soil-an experimental approach. *Geotech. Test. J.* 40 (6), 1026–1042. https://doi.org/10.1520/GTJ20160145.

Mehdizadeh, A., Disfani, M.M., Evans, R., Arulrajah, A., 2017b. Progressive internal erosion in a gap-graded internally unstable soil: Mechanical and geometrical effects. *Int. J. Geomech.* 18 (3). https://doi.org/10.1061/(ASCE)GM.1943-5622.0001085 04017160.

Mehdizadeh, A., Disfani, M.M., Evans, R., Arulrajah, A., 2019. Impact of suffusion on the cyclic and post-cyclic behaviour of an internally unstable soil. *Géotech. Lett.* 9 (3), 218–224. https://doi.org/10.1680/jgele.18.00128.

Muir Wood, D., Maeda, K., Nukudani, E., 2010. Modelling mechanical consequences of erosion. *Géotechnique* 60 (6), 447–457. https://doi.org/10.1680/geot.2010.60.6.447.

Okamura, M., Tsuyuguchi, Y., Izumi, N., Maeda, K., 2022. Centrifuge modeling of scale effect on hydraulic gradient of backward erosion piping in uniform aquifer under river levees. *Soils Found.* 62 (5). https://doi.org/10.1016/j.sandf.2022.101214 101214.

Ouyang, M., Takahashi, A., 2016. Influence of initial fines content on fabric of soils subjected to internal erosion. *Can. Geotech. J.* 53 (2), 299–313. https://doi.org/10.1139/cgj-2014-0344.

Ovalle-Villamil, W., Sasanakul, I., 2021. Centrifuge modeling study of backward erosion piping with variable exit size. *J. Geotech. Geoenviron. Eng.* 147 (11). https://doi.org/10.1061/(ASCE)GT.1943-5606.0002642 04021114.

Ovalle-Villamil, W., Sasanakul, I., 2022. Influence of seepage length on backward erosion piping behaviors in centrifuge model testing. *J. Geotech. Geoenviron. Eng.* 148 (11). https://doi.org/10.1061/(ASCE)GT.1943-5606.0002916 04022102.

Peng, S., Rice, J.D., Zhang, W., Luo, G., Cao, H., Pan, H., 2024. Laboratory investigation of the effects of blanket defect size on initiation of backward erosion piping. *J. Geotech. Geoenviron. Eng.* 150 (10). https://doi.org/10.1061/JGGEFK.GTENG-11976 04024095.

Pol, J.C., Kanning, W., van Beek, V.M., Robbins, B.A., Jonkman, S.N., 2022. Temporal evolution of backward erosion piping in small-scale experiments. *Acta Geotech.* 17 (10), 4555–4576. https://doi.org/10.1007/s11440-022-01545-1.

Prasomsri, J., Takahashi, A., 2020. The role of fines on internal instability and its impact on undrained mechanical response of gap-graded soils. *Soils Found.* 60 (6), 1468–1488. https://doi.org/10.1016/j.sandf.2020.09.008.

Prasomsri, J., Takahashi, A., 2021. Experimental study on suffusion under multiple seepages and its impact on undrained mechanical responses of gap-graded soil. *Soils Found.* 61 (6), 1660–1680. https://doi.org/10.1016/j.sandf.2021.10.003.

Richards, K.S., Reddy, K.R., 2012. Experimental investigation of initiation of backward erosion piping in soils. *Géotechnique* 62 (10), 933–942. https://doi.org/10.1680/geot.11.P.058.

Robbins, B.A., van Beek, V.M., Lopez-Soto, J.F., Montalvo-Bartolomei, A.M., Murphy, J., 2018. A novel laboratory test for backward erosion piping. *Int. J. Phys. Model. Geotech.* 18 (5), 266–279. https://doi.org/10.1680/jphmg.17.00016.

Sakai, K., Araki, G., Murono, Y., 2017. Equivalent single degree of freedom method for nonlinear dynamic analysis of embankment. *J. Jpn. Soc. Civ. Eng.*, Ser. A1 73 (1), 174–186. https://doi.org/10.2208/jscejseee.73.174.

Takahashi, A., Yamagata, S., Inoue, T., Horikoshi, K., 2024. Shake table tests on levees deteriorated by seepage-induced internal erosion in geotechnical centrifuge. *Jpn. Geotech. Soc. Spec. Publ.* 10 (33), 1270–1273. https://doi.org/10.3208/jgssp.v10.OS-22-06.

Takemura, J., Kondoh, M., Esaki, T., Kouda, M., Kusakabe, O., 1999. Centrifuge model tests on double propped wall excavation in soft clay. *Soils Found.* 39 (3), 75–87. https://doi.org/10.3208/sandf.39.3_75.

Takizawa, A., Horikoshi, K., Takahashi, A., 2018. Physical modelling of backward erosion piping in layered levee foundation. In: Keh-Chia, Y. (Ed.), Scour and Erosion IX: Proceedings of the 9th International Conference on Scour and Erosion (ICSE 2018), November 5–8, 2018, Taipei, Taiwan. CRC Press, pp. 33–38. https://doi.org/10.1201/9780429020940.

Taylor, D.W., 1948. Fundamentals of Soil Mechanics. John Wiley & Sons, New York (Chapter 6). ISBN-13: 978-1258768928.

van Beek, V.M., van Essen, H.M., Vandenboer, K., Bezuijen, A., 2015. Developments in modelling of backward erosion piping. *Géotechnique* 65 (9), 740–754. https://doi.org/10.1680/geot.14.P.119.

van Genuchten, M., 1980. A closed-form equation for predicting the hydraulic conductivity of unsaturated soils. *Soil Sci. Soc. Am. J.* 44, 892–898. https://doi.org/10.2136/sssaj1980.03615995004400050002x.

Vandenboer, K., van Beek, V.M., Bezuijen, A., 2018. 3D character of backward erosion piping. *Géotechnique* 68 (1), 86–90. https://doi.org/10.1680/jgeot.16.P.091.

Wang, G., Horikoshi, K., Takahashi, A., 2021. Effects of internal erosion on parameters of subloading Cam-clay model. *Geotech. Geol. Eng.* 38 (2), 1323–1335. https://doi.org/10.1007/s10706-019-01093-8.

Xiao, M., Shwiyhat, N., 2012. Experimental investigation of the effects of suffusion on physical and geomechanic characteristics of sandy soils. *Geotech. Test. J.* 35 (6), 890–900. https://doi.org/10.1520/GTJ104594.

Xu, J., Ueda, K., Uzuoka, R., 2022. Evaluation of failure of slopes with shaking-induced cracks in response to rainfall. *Landslides* 19 (1), 119–136. https://doi.org/10.1007/s10346-021-01734-1.